Chinese Chemical Letters 35 (2024) 108950

Contents lists available at ScienceDirect

Chinese Chemical Letters

journal homepage: www.elsevier.com/locate/cclet

Pyridapeptides F–I, cyclohexapeptides from marine sponge-derived *Streptomyces* sp. OUCMDZ-4539

Shuige Zhao[a,1], Pengcheng Yan[a,1], Peipei Liu[a], Haishan Liu[c], Ning Li[d], Peng Fu[a,b,*], Weiming Zhu[a,b,*]

[a] Key Laboratory of Marine Drugs, Ministry of Education of China, School of Medicine and Pharmacy, Ocean University of China, Qingdao 266003, China
[b] Key Laboratory for Marine Drugs and Bioproducts, Laoshan Laboratory, Qingdao 266237, China
[c] School of Biological Science and Technology, University of Jinan, Ji'nan 250022, China
[d] Key Laboratory for Biosensors of Shandong Province, Biology Institute, Qilu University of Technology, Ji'nan 250103, China

ARTICLE INFO

Article history:
Received 27 June 2023
Revised 17 August 2023
Accepted 18 August 2023
Available online 19 August 2023

Keywords:
Marine microorganism
Streptomyces
Cyclopeptide glycosides
Pyridapeptides
Antiproliferative activity

ABSTRACT

Four new cyclohexapeptides, pyridapeptides F–I (**1**–**4**), were isolated from the fermentation broth of marine sponge-derived *Streptomyces* sp. OUCMDZ-4539. The pyridapeptides F–H (**1**–**3**) are composed of β-hydroxyleucine, alanine, *O*-methylthreonine, hexahydropyridazine-3-carboxylic acid, 5-hydroxytetrahydropyridazine-3-carboxylic acid, and (2*S*,3*R*,4*E*,6*E*)-2-amino-3–hydroxy-4,6-dienoic acid residues. Pyridapeptide I (**4**) contains (2*S*,3*R*,4*E*,6*E*)-2-amino-3–hydroxy-8-methylnona-4,6-dienoic acid residue and a very rare glycose residue, aculose. Their structures were determined based on spectroscopic analysis and chemical methods. Pyridapeptides G–I (**2**–**4**) have the 2,3,6-trideoxyhexose units glycosylated at the γ-OH-TPDA residue, displayed significant antiproliferative activity against four (PC9, MKN45, HepG2, K562) or two (PC9, MKN45) human cancer cell lines.

Over 120 cyclopeptides that contain hexahydropyridazine-3-carboxylic acid (HPDA) have been reported [1], including piperazimycin A [2], hytramycin V [3], and soliseptide A [4]. These molecules, in general, show strong bioactivities, including cytotoxic, antimicrobial and antiviral activities [1]. The cytotoxic and antibacterial activities of 7-*O*-L-rhodosamine- or rhodinose-bearing anthracyclines significantly increased compared to the aglycone [5,6], indicating that bioactivity of the aglycone could be improved by glycosylation. Our group has isolated five HPDA-containing cyclohexapeptides, pyridapeptides A–E, from the marine sponge-derived *Streptomyces* strain OUCMDZ-4539, among which pyridapeptides B–E bearing one or more 2,3,6-trideoxyhexose residues displayed significant antiproliferative activity [7]. These reports indicated that oligosaccharide chains were important for antiproliferative activity. To obtain diverse pyridapeptide analogs containing sugar lotus, we re-fermented the strain OUCMDZ-4539 in a large amount of liquid media and examined various secondary metabolites. As a result, we identified four new cyclohexapeptides, pyridapeptides F–I (**1**–**4**) (Fig. 1).

Pyridapeptide F (**1**) was obtained as a white solid. The molecular formula was determined to be $C_{33}H_{52}O_{10}N_8$ with an index of hydrogen deficiency (IHD) of 11 from the high resolution electrospray ionization mass spectroscopy (HRESIMS) peak at *m/z* 719.3715 $[M-H]^-$ (calcd. 719.3734) (Fig. S15 in Supporting information). The relationships between the specific proton and carbon signals in the ^1H and ^{13}C nuclear magnetic resonance (NMR) data of compound **1** were established by the heteronuclear singular quantum correlation (HSQC) spectrum. Six downfield carbon signals for the amide or ester carbonyl groups at δ_C 169.6, 169.7, 170.0, 171.0, 171.2, and 171.3 as well as six α-amino acid methine carbons at δ_C 48.3, 49.5, 50.0, 53.4, 55.9, and 56.1 were observed in the ^{13}C NMR spectrum. Meanwhile, four amide proton signals at δ_H 8.40, 8.31, 8.06, and 7.59 were observed in the ^1H NMR spectrum (Table 1), revealing that **1** should be a hexapeptide.

Analyses of the ^1H–^1H correlation spectroscopy (COSY) and heteronuclear multiple bond correlation (HMBC) spectra revealed six partial structures, as shown in Fig. 2. The ^1H–^1H COSY and total correlation spectroscopy (TOCSY) correlations of HN-2 (δ_H 8.06)/H-2/H-3/H-4/H-5/H-6/H-7/H_2-8/H_3-9 and the HMBC correlations of the α-methine H-2 (δ_H 4.42) to C-1 (δ_C 169.6) showed the presence of the 2-amino-3-hydroxynona-4,6-dienoic acid (AHNA) residue. The ^1H–^1H COSY and TOCSY correlations of HN-11 (δ_H 8.31)/H-11/H-12/H-13/H_3-14 (H_3-15) and the HMBC

* Corresponding authors.
E-mail addresses: fupeng@ouc.edu.cn (P. Fu), weimingzhu@hotmail.com (W. Zhu).
[1] These authors contributed equally to this work.

https://doi.org/10.1016/j.cclet.2023.108950
1001-8417/

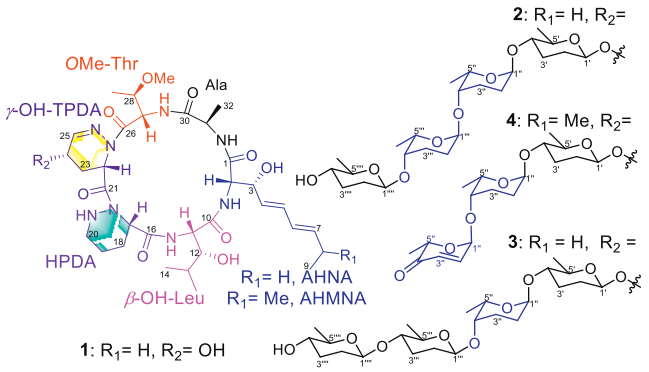

Fig. 1. Structures of compounds **1**–**4**.

Table 1
^{1}H (500 MHz) and ^{13}C (150 MHz) NMR data for pyridapeptide F (**1**) in DMSO–d_6.

Position	δ_C	δ_H, mult. (J in Hz)
AHNA		
1	169.6, C	
2	55.9, CH	4.42, dd (9.0, 4.0)
2-NH		8.06, d (9.0)
3	71.8, CH	4.39, m
4	131.5, CH	5.47, dd (15.0, 5.2)
5	130.0, CH	6.10, dd (15.0, 10.6)
6	128.7, CH	5.95, dd (15.2, 10.6)
7	135.3, CH	5.67, dd (15.2, 6.5)
8	25.1, CH_2	2.05, m
9	13.4, CH_3	0.95, d (7.5)
β-OH-Leu		
10	170.0, C	
11	56.1, CH	4.24, m
11-NH		8.30, d (7.9)
12	73.9, CH	3.46, m
13	29.2, CH	1.53, m
14	20.2, CH_3	0.80, d (7.2)
15	16.0, CH_3	0.81, d (7.2)
HPDA		
16	171.0, C	
17	50.0, CH	4.80, d (5.2)
18	25.6, CH_2	2.04, m; 1.75, m
19	20.9, CH_2	1.47, m
20	46.6, CH_2	3.07, d (13.2); 2.65, m
20-NH		5.14, d (13.2)
γ-OH-TPDA		
21	171.3, C	
22	49.5, CH	5.72, dd (2.2, 6.2)
23	27.3, CH_2	2.18, dd (6.4, 13.0); 1.79, m
24	59.0, CH	4.00, dd (6.6, 11.4)
25	146.9, CH	6.83, s
OMe-Thr		
26	169.7, C	
27	53.4, CH	5.17, dd (2.8, 9.0)
27-NH		7.59, d (9.0)
28	76.7, CH	3.82, dq (2.8, 6.3)
28-OCH_3	56.5, CH_3	3.16, s
29	15.9, CH_3	1.02, d (6.3)
Ala		
30	171.2, C	
31	48.3, CH	4.27, dq (6.9, 7.0)
31-NH		8.40, d (6.9)
32	15.9, CH_3	1.17, d (6.9)

correlations of the α-methine H-11 (δ_H 4.24) to C-10 (δ_C 170.0) showed the presence of a β-hydroxyleucine (β-OH-Leu) moiety. The proximity of the α-methine H-17 (δ_H 4.80) to HN-20 (δ_H 5.14) through H_2-18 (δ_H 1.75/2.04), H_2-19 (δ_H 1.47), and H_2-20 (δ_H 2.65/3.07) in the COSY and the correlations of H-17 (δ_H 4.80) to C-16 (δ_C 171.0) in the HMBC suggested the presence of an HPDA residue. The ^{1}H–^{1}H COSY spin system from the α-methine H-22 (δ_H 5.72) to H-25 (δ_H 6.83) and the

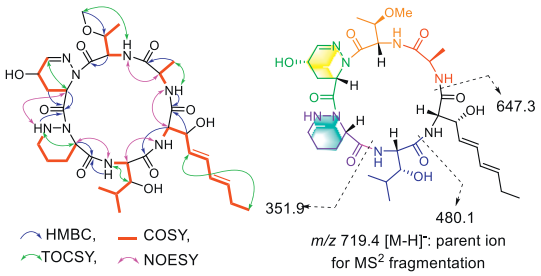

Fig. 2. Key 2D NMR correlations and MS^2 fragmentation of **1**.

HMBC from H-22 to C-21 (δ_C 171.3) together with the chemical shifts of CH-24 ($\delta_{H/C}$ 4.00/59.0) and CH-25 ($\delta_{H/C}$ 6.83/146.9) suggested the presence of a 5-hydroxytetrahydropyridazine-3-carboxylic acid (γ-OH-TPDA) residue. The ^{1}H–^{1}H COSY and TOCSY correlations of HN-27 (δ_H 7.59)/H-27/H-28/H_3-29 and the HMBC correlations of the α-methine H-27 (δ_H 5.17) to C-26 (δ_C 169.7) and 28-OCH_3 (δ_H 3.16) to C-28 (δ_C 76.7) showed the presence of an *O*-methylthreonine (*O*Me-Thr) moiety. The ^{1}H–^{1}H COSY correlations of 31-NH (δ_H 8.40)/H-31/H_3-32 and the HMBC correlations of H-31/H_3-32 to C-30 (δ_C 171.2) indicated the presence of an alanine (Ala) moiety. The connectivity among these residues was established, as showing in Fig. 2, by the key HMBC correlations from H-2 of AHNA to C-10 of β-OH-Leu, HN-11 of β-OH-Leu-to C-16 of HPDA, HN-20 of HPDA to C-21 of γ-OH-TPDA, and HN-31 of Ala to C-1 of AHNA as well as the key NOESY correlations between HN-2 of AHNA and H-11 of β-OH-Leu, HN-11 of β-OH-Leu and H-17 of HPDA, HN-20 of HPDA and H-22 of γ-OH-TPDA, HN-27 of *O*Me-Thr and H-31 (δ_H 4.27) of Ala, HN-31 of Ala and H-2 of AHNA. These results revealed that compound **1** was an undocumented cyclohexapeptide, namely *cyclo*-(AHNA-(β-OH-Leu)-HPDA-(γ-OH-TPDA)-(*O*Me-Thr)-Ala). The suggested sequence was further confirmed by the positive ESI-MS^2 fragment ion series at *m/z* 719.4, 647.3, 480.1 and 351.9 $[M-H]^-$ corresponding to the parent and fragment ions by the loss of Ala, AHNA, and β-OH-Leu in turn. Both Δ^4 and Δ^6 double-bond geometries of the AHNA residue were assigned as *E*- by 15.0 Hz and 15.2 Hz of the ^{3}J coupling constants.

The absolute configuration of compound **1** was determined as follows, among which the Ala, *O*Me-Thr, HPDA and β-OH-Leu residues of **1** were found by the advanced Marfey's method using L- and D-*N*-(5-fluoro-2,4-dinitrophenyl)valinamide (FDVA) [8,9]. The results indicated that compound **1** contained D-Ala, L-HPDA (Fig. S2 in Supporting information), (*R*)-*O*Me-L-Thr and (3*R*)-OH-L-Leu (Fig. S3 in Supporting information). The *cis*- configuration of γ-OH-TPDA was assigned according to the nuclear overhauser effect spectroscopy (NOESY) correlation of H-22 and H-24 and was further determined to be (*S*,*S*)- after elucidating 24-OH as the *S*-configuration by Mosher's method (Fig. 3). The configuration of

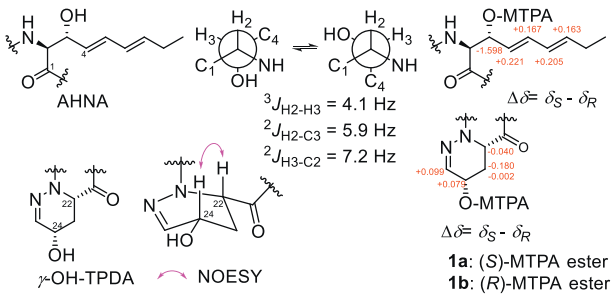

Fig. 3. Configurations of AHNA and γ-OH-TPDA units of **1**.

AHNA was elucidated as *threo*– by the heteronuclear single quantum multiple bond correlation (HSQMBC) spectrum [10] that gave $^{3}J_{H2\text{-}H3}$, $^{2}J_{H2\text{-}C3}$ and $^{2}J_{H3\text{-}C2}$ values of 4.1, 5.9 and 7.2 Hz, and further determined as having an (*S*,*R*)- configuration by Mosher's method (Fig. 3) [7].

Both pyridapeptides G (**2**) and H (**3**) provided compound **1** following mild hydrolysis with 0.5 mol/L HCl under an argon atmosphere (Fig. S4 in Supporting information), indicating that they shared the same pyridapeptide F (**1**) backbone. The molecular formula of pyridapeptide G (**2**) was determined to be $C_{57}H_{92}O_{18}N_8$ by HRESIMS at *m/z* 1175.6455 $[M–H]^-$ (calcd. 1175.6446) (Fig. S33 in Supporting information), with a molecular weight of 114 × 4 amu higher than that of pyridapeptide F (**1**), implying four extra trideoxyhexose residues. Apart from the NMR signals for cyclic hexapeptide (**1**), the ^{1}H and ^{13}C NMR data of compound **2** (Table S2 in Supporting information) contained 24 extra carbon signals that were classified by the HSQC spectrum as four acetal methines ($\delta_{C/H}$ 100.5/4.75, CH-1′; $\delta_{C/H}$ 98.2/4.79, CH-1″; $\delta_{C/H}$ 98.6/4.69, CH-1‴; $\delta_{C/H}$ 103.0/4.39, CH-1⁗), eight oxymethines ($\delta_{C/H}$ 78.1/3.06, CH-4′; 73.9/3.38, CH-5′; $\delta_{C/H}$ 74.8/3.44, CH-4″; 66.2/3.81, CH-5″; $\delta_{C/H}$ 66.2/3.38, CH-4‴; 66.7/3.80, CH-5‴; $\delta_{C/H}$ 75.5/3.11, CH-4⁗; 70.0/4.33, CH-5⁗), eight methylenes ($\delta_{C/H}$ 30.4/1.83&1.40, CH_2–2′; 29.1/1.98&1.52, CH_2–3′; $\delta_{C/H}$ 30.7/1.82 &1.40, CH_2–2″; 24.1/1.78&1.48, CH_2–3″; $\delta_{C/H}$ 24.0/1.80&1.40, CH_2–2‴; 24.4/1.83&1.40, CH_2–3‴; $\delta_{C/H}$ 24.6/1.80&1.38, CH_2–2⁗; 31.1/1.81&1.31, CH_2–3⁗), and four methyls ($\delta_{C/H}$ 17.0/1.12, CH_3–6′; $\delta_{C/H}$ 18.2/1.10, CH_3–6″; $\delta_{C/H}$ 17.0/0.96, CH_3–6‴; $\delta_{C/H}$ 18.4/0.99, CH_3–6⁗). In addition, the ^{1}H–^{1}H COSY spectrum displayed correlations from H-1′ to H-6′, H-1″ to H-6″, H-1‴ to H-6‴ and H-1⁗ to H-6⁗ in sequence. These data presented the four trideoxyhexose residues as the 2,3,6-trideoxyhexoses, implying that compound **2** was a tetraglycoside of pyridapeptide F (**1**) and further confirmed by MS^2 analysis (Fig. S44 in Supporting information). The NOESY correlations (Fig. S9 in Supporting information) of H-1′ (δ_H 4.75) with H-5′ (δ_H 3.38), H-4″ (δ_H 3.44) with H_3–6″ (δ_H 1.10), H-4‴ (δ_H 3.38) with H_3–6‴ (δ_H 0.96) and H-1⁗ (δ_H 4.40) with H-5⁗ (δ_H 4.33) respectively suggested the *trans*-H-1′/H_3–6′, *cis*-H-4″/H_3–6″, *cis*-H-4‴/H_3–6‴, and *trans*-H-1⁗/H_3–6⁗ orientations, indicating that these 2,3,6-trideoxyhexoses could be amicetose, rhodinose, rhodinose and amicetose in sequence. This deduction was then confirmed by the complete hydrolysis of compound **2** in 2 mol/L HCl at 90 °C followed by hydrazonation with 2,4-dinitrophenylhydrazine that yielded equal amounts of D-amicetose-2,4-dinitrophenylhydrazone (**6**) and L-rhodinose-2,4-dinitrophenylhydrazone (**7**), both detected at *m/z* 311 $[M–H]^-$ (Figs. S7 and S8 in Supporting information), as identified by NMR (Table S2), LC-MS (Fig. S6 in Supporting information) and specific rotation ($[\alpha]_D^{20}$ −9.2 *vs.* −10.0 (*c* 0.15, pyridine) for **6** and −21.5 *vs.* −21.4 (*c* 0.14, pyridine) for **7**) [7]. Furthermore, the NOESY correlation from the anomeric proton H-1″ (δ_H 4.79) to H-4′ (δ_H 3.06), H-1‴ (δ_H 4.69) to H-4″ (δ_H 3.44), and H-1⁗ (δ_H 4.39) to H-4‴ (δ_H 3.38) completed the connectivity of these monosaccharides linked into a tetrasaccharide by three 1,4-glycosidic bonds. The key NOESY correlation of the anomeric proton H-1′ (δ_H 4.75) with H-24 (δ_H 4.11) of the γ-OH-TPDA residue, as well as the values of $\delta_{C\text{-}24}$ and $\delta_{C\text{-}25}$ of compound **2** that were respectively 7.0 ppm increase and 3.8 ppm decrease when compared to compound **1**, indicated that the glycosidation occurred at 24-OH of the cyclic hexapeptide. The $^{1}J_{C\text{-}H}$ values for CH-1′, 1″, 1‴, and 1⁗ were respectively measured as 153, 170, 165 and 152 Hz (Fig. S43 in Supporting information), suggesting the axial orientations for both H-1′ and H-1⁗, and equatorial orientations for both H-1″ and H-1‴ [7]. That is β-anomer for both D-amicetoses and α-anomer for both L-rhodinoses. Consequently, pyridapeptide G (**2**) was elucidated as 24-*O*-(β-D-amicetopyranosyl-(1→4)-α-L-rhodinopyranosyl-(1→4)-α-L-rhodinopyranosyl-(1→4)-β-D-amicetopyranosyl) pyridapeptide F.

Pyridapeptide H (**3**) was an isomer of **2** based on the same molecular formula from the HRESIMS peak at *m/z* 1175.6404 $[M–H]^-$ (calcd. 1175.6446) (Fig. S45 in Supporting information) and MS^2 analysis (Fig. S56 in Supporting information). Comparison of the ^{1}H, ^{13}C NMR (Table S3 in Supporting information), and NOESY (Fig. S9) spectra of **3** with those of **2** revealed a difference in that an amicetose residue in **3** replaced the corresponding rhodinose residue in **2**. The same thermal acidolysis of **3** followed by a similar hydrazonation as for **2** yielded a 3:1 ratio of compounds **6** and **7** (Figs. S7 and S8) and specific rotations, further confirming this deduction. The NOESY correlations of H-1‴ (δ_H 4.46) to H-4″ (δ_H 3.45) and H-5‴ (δH 3.10) (Fig. S9) suggested that the third hexose residue of **2**, L-rhodinose, was replaced by the D-amicetose in **3**. The 155 Hz of $^{1}J_{C\text{-}H}$ value for CH-1‴ suggested a β-anomeric center (Fig. S55 in Supporting information). Thus, pyridapeptide H (**3**) was elucidated as 24-*O*-(β-D-amicetopyranosyl-(1→4)-β-D-amicetopyranosyl-(1→4)-α-L-rhodinopyranosyl-(1→4)-β-D-amicetopyranosyl) pyridapeptide F.

Pyridapeptide I (**4**) provided pyridapeptide A (**5**) (Fig. S10 in Supporting information) following mild hydrolysis with 0.5 mol/L HCl under an argon atmosphere (Fig. S3), indicating that they shared the same cyclohexapeptide backbone [7]. The molecular formula of **4** was determined to be $C_{52}H_{80}O_{16}N_8$ based on the HRESIMS at *m/z* 1071.5588 $[M–H]^-$ (calcd. 1071.5614) (Fig. S57 in Supporting information) with 110 amu higher than pyridapeptide C, a new bioside [7]. The NMR data (Table S4 in Supporting information) of compound **4** exhibited a high degree of similarity to that of pyridapeptide C [7], supporting a 2-amino-3–hydroxy-8-methylnona-4,6-dienoic acid (AHMNA) residue in compound **4**. A thorough analysis of 1D NMR and examining the NOESY of **4** (Fig. S9) revealed an additional six-carbon fragment than pyridapeptide C. This fragment contained by the HSQC spectrum an acetal methine ($\delta_{C/H}$ 94.7/5.33, CH-1⁗), two olefinic methines ($\delta_{C/H}$ 145.0/7.07, CH-2⁗; $\delta_{C/H}$ 126.2/6.08, CH-3⁗), a carbonyl (δ_C 196.9, CH-4⁗), an oxymethine ($\delta_{C/H}$ 69.7/4.51, CH-5⁗), and a methyl group ($\delta_{C/H}$ 15.2/1.23, CH_3–6⁗). This additional sugar moiety was further determined as an aculose residue according to the ^{1}H–^{1}H COSY correlations from H-1‴ to H-3‴ *via* H-2‴ as well as the NOESY correlation of H-3‴ (δ_H 6.08) with H-5‴ (δ_H 4.51) (Fig. S9). And the small coupling constant of H-1‴ (3.5 Hz) was consistent with the α-anomer [11]. The same thermal acidic hydrolysis of **4** followed by a similar hydrazonation as for **1** yielded a 1:1 ratio of compounds **6** and **7** (Fig. S6). Consequently, pyridapeptide I (**4**) was elucidated as 4″-*O*-α-L-aculosylpyridapeptide C after combination of the MS^2 analysis (Fig. S68 in Supporting information).

Compounds **1**–**4** were evaluated for their antiproliferative activity against PC9, MKN45, HepG2, K562, L-02 cell lines by the cell counting kit-8 (CCK-8) assay [12,13] using adriamycin as the positive control. The results (Table S5 in Supporting information) showed that compounds **2** and **3** bearing linear tetrasaccharide chains exhibited a broad-spectrum of antiproliferative activity against the five human cell lines with the values of 50% inhibitory concentration (IC_{50}) ranging from 1.33 μmol/L to 3.33 μmol/L, while compound **4** having a trisaccharide chain showed a selective antiproliferation against the human lung cancer cell line (PC9) and human hepatoma cell line (HepG2) with IC_{50} value of 3.39 μmol/L and 3.04 μmol/L, respectively. Cyclohexapeptide (**1**) was no significant activity against the proliferation of the five cell lines (IC_{50} > 10 μmol/L). These data combined with our published results [7] indicated that the linear tetraglycosides, compounds **2** and **3** as well as pyridapeptides D and E (Fig. S10), all showed a broad-spectrum of antiproliferative activity against all the tested human cells, while

the diglycoside, pyridapeptide C, and the linear triglycoside **4** displayed a selective antiproliferation against one or two human tumor cells. However, the aglycone, compound **1** and pyridapeptide A as well as the monoglycoside, pyridapeptide B (Fig. S10), did not show bioactivity against the proliferation of the cell lines (IC_{50} > 10 μmol/L), indicating that the oligosaccharide modification significantly increases the antiproliferation of these cyclohexapeptides. Our results again confirmed that marine-derived microorganisms are an important source of bioactive natural products [14,15].

Declaration of competing interest

The authors declare that they have no known competing financial interests or personal relationships that could have appeared to influence the work reported in this paper.

Acknowledgments

This work was financially supported by the National Natural Science Foundation of China (No. U1906213) and the National Key Research and Development Program of China (No. 2022YFC2804100).

Supplementary materials

Supplementary material associated with this article can be found, in the online version, at doi:10.1016/j.cclet.2023.108950.

References

[1] K.D. Morgan, R.J. Andersen, K.S. Ryan, Nat. Prod. Rep. 36 (2019) 1628–1653.
[2] E.D. Miller, C.A. Kauffman, P.R. Jensen, W. Fenical, J. Org. Chem. 72 (2007) 323–330.
[3] G. Cai, J.G. Napolitano, J.B. Mcalpine, et al., J. Nat. Prod. 76 (2013) 2009–2018.
[4] J. Wang, Z. Cong, X. Huang, et al., Org. Lett. 20 (2018) 1371–1374.
[5] C. Gui, J. Yuan, X. Mo, et al., J. Nat. Prod. 81 (2018) 1278–1289.
[6] C. Cui, J. Chen, Q. Xie, et al., J. Commun. Biol. 2 (2019) 454.
[7] S. Zhao, Y. Xia, H. Liu, et al., Org. Lett. 24 (2022) 6750–6754.
[8] P. Fu, M. Jamison, S. La, J.B. MacMillan, Org. Lett. 16 (2014) 5656–5659.
[9] H. Zhou, Y.B. Yang, R.T. Duan, et al., Chin. Chem. Lett. 27 (2016) 1044–1047.
[10] N. Matsumori, D. Kaneno, M. Murata, H. Nakamura, K. Tachibana, J. Org. Chem. 64 (1999) 866–876.
[11] I. Voitsekhovskaia, C. Paulus, C. Dahlem, et al., Microorganisms 8 (2020) 680.
[12] M. Lan, T. Cui, K. Xia, et al., Chin. Chem. Lett. 33 (2022) 508–510.
[13] H. Chen, F. Xu, B.B. Xu, et al., Chin. Chem. Lett. 27 (2016) 277–282.
[14] C.L. Xie, D. Zhang, K.Q. Guo, et al., Chin. Chem. Lett. 33 (2022) 2057–2059.
[15] F. Li, W. Sun, S. Zhang, et al., Chin. Chem. Lett. 31 (2020) 197–201.